

## STUDY ON FORMULATION OF BACTERIAL CELLULOSE NANOFIBERS-COATED NANOLIPOSOMES CONTAINING PACLITAXEL FOR ORAL ADMINISTRATION

CUONG BA CAO<sup>1</sup>, PHONG XUAN ONG<sup>2</sup>, THANH XUAN NGUYEN<sup>1\*</sup>

<sup>1</sup>Faculty of Biology and Agricultural Engineering, Hanoi Pedagogical University 2, Xuan Hoa Ward, Phuc Yen City, Vinh Phuc Province-280000, Viet Nam. <sup>2</sup>Institute of Scientific Research and Applications, Hanoi Pedagogical University 2, Xuan Hoa Ward, Phuc Yen City, Vinh Phuc Province-280000, Viet Nam

\*Corresponding author: Thanh Xuan Nguyen; \*Email: nguyensexuanthanh@hpu2.edu.vn

Received: 06 Dec 2023, Revised and Accepted: 17 Jan 2024

### ABSTRACT

**Objective:** The low oral bioavailability of paclitaxel (PAC) because of its limited aqueous solubility and poor intestinal permeability after being administered orally suggests the need for a sustained release system. The aim of this study is to produce and evaluate *in vitro* a nanoliposome system that carries paclitaxel (BCN-LIP-PAC) for oral administration.

**Methods:** Thin-film evaporation and electrostatic deposition methods were used to obtain LIP-PAC and BCN-LIP-PAC. Particle size, polydispersity index (PDI), zeta potential, morphological analysis, entrapment efficiency percentage (EE%), and *in vitro* dissolution studies were used to characterize the developed systems.

**Results:** The nano-range sizes of LIP-PAC and BCN-LIP-PAC (0.1 % BCN) were 112±4.2 nm and 154±6.4 nm, respectively, where EE % were 80.6±2.3 % and 84.6±1.7 %, respectively. BCN-LIP-PAC exhibited good stability in simulated gastrointestinal fluids. The drug release experiments conducted *in vitro* showed that BCN-LIP-PAC had obvious sustained release behaviors when compared to LIP-PAC. Furthermore, the release rate of PAC from all LIP-PAC and BCN-LIP-PAC was higher in SIF than in SGF.

**Conclusion:** The preparation, characterization, and evaluation of BCN-LIP-PAC (0.1 % BCN) for oral PAC delivery were all successful. In conclusion, the approach presented herein is a promising option for delivering oral sustained-release PAC.

**Keywords:** Bacterial cellulose nanofibers-coated nanoliposomes, Paclitaxel, Oral administration

© 2024 The Authors. Published by Innovare Academic Sciences Pvt Ltd. This is an open access article under the CC BY license (<https://creativecommons.org/licenses/by/4.0/>)  
DOI: <https://dx.doi.org/10.22159/ijap.2024v16i2.50056> Journal homepage: <https://innovareacademics.in/journals/index.php/ijap>

### INTRODUCTION

Drug carriers typically use oral administration as one of their preferred and traditional methods. Safety, simplicity, convenience, and high patient compliance are the main advantages of this drug delivery carrier, which increase the therapeutic efficacy of the drug [1]. The risk of disease transmission can be minimized, costs can be reduced, and dosing frequency can be more flexible or controlled with oral administration [2]. Despite its ability to safely, selectively, and effectively absorb many nutrients, the gastrointestinal (GI) tract creates a physical barrier for drug absorption [2]. Due to the physicochemical properties of drugs and physiological barriers like GI instability, oral administration of many drugs poses a significant challenge [1]. Many promising applications exist for nano-delivery systems in enhancing the oral bioavailability of drugs [3, 4].

One of the most widely utilized and effective cancer drugs is paclitaxel (PAC). A wide range of cancers can be effectively treated with it, such as ovarian and breast cancers, head and neck cancers, colon cancer, and others [5, 6]. It is unfortunate that PAC is difficult to administer orally because it has a low oral bioavailability [7, 8]. In order to overcome PAC's limited aqueous solubility, organic solvents are used as pharmaceutical excipients in the intravenous formulation. The use of organic solvents in the intravenous formulation can result in side effects like hypersensitivity reactions [6]. Several attempts have been made to develop oral PAC formulations to reduce its toxicity and increase its oral bioavailability, taking into account the various advantages of administering it orally [9-14].

Liposomes (LIP) are commonly employed in the delivery of bioactive agents to cells and tissues while shielding them from physiological barriers [15-17]. The use of LIP, a promising nanocarrier, has resulted in superior benefits in improving oral drug bioavailability by encapsulating drugs into lipid bilayers, which has improved their aqueous solubility [18]. Conventional LIPs are made up of concentric layers of phospholipids and can be damaged by harsh chemical and enzyme environments in the GI tract, resulting in decreased oral

bioavailability [1, 15]. The surface of LIP has been modified to improve their oral stability and functionalize it, and various attempts have been made to overcome these problems. The incorporation of surfactants, such as bile salts, has caused many modifications to this surface [19], or by coating functional polymers such as chitosan [20-28] and polyethylene glycol (PEG) [29, 30], or by the designing of multilayered or multi-vesicular carriers [30-32].

By adding chitosan to liposomes, their stability in various biological fluids, such as simulated gastric fluid (SGF) and intestinal fluid (SIF), can be enhanced. Chitosan-coated products can have an increased mucoadhesive properties, cellular uptake, and solubility of drugs [20-28]. Chitosan is well-known for its biopharmaceutical properties, which include nontoxicity, biocompatibility, biodegradability, and mucoadhesion. Chitosan has been widely accepted in biomedical and biotechnological fields due to its capacity to open epithelial tight junctions and its FDA-GRAS status [19]. To enhance the solubility and paracellular transport of numerous drugs, including curcumin [20, 22-24, 26], berberine hydrochloride [21], furosemide [25], and other ones, chitosan has been employed to coat liposomes.

In addition, bacterial cellulose (BC) is a biodegradable polymer that is made through biological pathways from bacteria in environments with different nutritional composition [4, 33]. BC is able to absorb and hold water well and has a network-like spatial structure that is made of many ultra-fine nanofibers [4, 34]. In the medical field, BC is a topic of interest and is utilized in mask preparations to moisturize the skin, adjuvants, artificial blood vessels for implanting, drug delivery systems, and burn treatment membranes [4, 35]. BC has been studied as a carrier and *in vitro* oral delivery of berberine [4]. Furthermore, BC is also a source of natural cellulose nanofibers [34]. Bacterial cellulose nanofibers (BCN) can be used to functionalize the surface of LIP to help protect Lip in an environment containing enzymes and pH of the gastrointestinal tract.

Our understanding is that the novelty of this design was that the oral drug delivery system of nanoliposomes with surface modification by

coating of bacterial cellulose nanofibers to provide an efficient way to deliver PAC through the oral route in the digestive tract. As a result, this delivery system has great potential for oral cancer treatment with PAC.

## MATERIALS AND METHODS

### Materials

Paclitaxel (purity  $\geq 97\%$ ), lecithin (purity  $\geq 60\%$  phosphatides), cholesterol (purity  $\geq 95\%$ ), and stearyl amine were purchased from Glentham Life Sciences Ltd (Corsham, United Kingdom). The purified bacterial cellulose pellicles were obtained from the results in our previous study [36]. Pancreatin and pepsin were purchased from Sigma-Aldrich (Missouri, USA). Dialysis bags (molecular weight cut-off, MWCO: 12 000-14 000) was purchased from Serva Electrophoresis GmbH (Hedelberg, Germany). NaCl, KCl, NaOH, HCl, and  $\text{H}_2\text{SO}_4$  were purchased from Samchun Chemical Co., Ltd (Seoul, Korea).  $\text{KH}_2\text{PO}_4$ ,  $\text{Na}_2\text{HPO}_4 \cdot 12\text{H}_2\text{O}$ , and  $\text{NaH}_2\text{PO}_4 \cdot 2\text{H}_2\text{O}$  were purchased from Daejung Chemicals and Metals Co., Ltd (Busan, Korea). Analytical grade was achieved by preparing all other reagents and buffer solution components.

### Methods

#### Preparation of nanoliposomes containing paclitaxel

Nanoliposomes containing paclitaxel (LIP-PAC) were prepared by thin film hydration technique followed by extrusion method [27, 28]. In brief, 49 mg lecithin, 23 mg cholesterol, 4 mg stearyl amine and 4 mg paclitaxel were dissolved in 50 ml mixture of chloroform and methanol (9:1 v/v) in a round bottom flask. Rotary evaporation (Daihan Scientific, Korea) of the organic solvents was used to produce the thin film. The traces of organic solvents were completely removed after drying a thin film in a vacuum oven at  $40\text{ }^\circ\text{C}$  for 4 h. PBS at pH 7.4 was used to hydrate the dry lipid film and vortexed until all components were dissolved. After hydration, the resulting multilamellar liposomal suspension was extruded through the combination of filters:  $0.8\text{ }\mu\text{m}$ ,  $0.45\text{ }\mu\text{m}$ ,  $0.22\text{ }\mu\text{m}$  and  $0.1\text{ }\mu\text{m}$  polycarbonate filters, to obtain LIP-PAC.

#### Preparation of bacterial cellulose nanofibers-coated nanoliposomes containing paclitaxel

By using acid hydrolysis, BC pellicles (from the results in our previous study [36]) were used to produce bacterial cellulose nanofibers (BCN) [34]. To summarize, the mechanical disintegration of the purified BC pellets into a cellulose paste was done using a blender at 5000 rpm for about 20 min under ambient temperature to pass through a 60-mesh screen. The CP was pressed to remove the majority of the water that had been absorbed. The acid solution was applied to the dried CP in a ratio of 1:10 g/ml and stirred continuously under various conditions as follows: the 65% (w/w)  $\text{H}_2\text{SO}_4$  solution at  $60\text{ }^\circ\text{C}$  for 2 h for  $\text{H}_2\text{SO}_4$  hydrolysis. An excess (10-fold) of cold deionized (DI) water was added to terminate the hydrolysis reactions. By centrifuging at 12 000 rpm for 10 min, the acidic solution was eliminated and the supernatant became turbid. The sediment was taken and filtered (MWCO: 12 000-14 000) with DI water until it attains neutral pH. Centrifugation for 20 min at 12 000 rpm and  $10\text{ }^\circ\text{C}$  was used to collect the BCN content after dialysis. To produce BCN suspensions of 0.33; 0.1; and 0.3% (w/v), the BCN samples were redistributed in DI water and ultrasonicated for 5 min before being used further.

Bacterial cellulose nanofibers-coated nanoliposomes containing paclitaxel (BCN-LIP-PAC) were prepared by the ionic interaction between LIP-PAC (positive charges [27, 28]) and BCN (negative charges [34]). To optimize the coating, 10 ml of BCN suspension at different concentrations (0.033, 0.1, 0.3%, w/v) were mixed with 10 ml of preformulated suspensions of nanoliposomes containing PAC under stirring at room temperature for 60 min.

#### Characterization of LIP-PAC and BCN-LIP-PAC

LIP-PAC and BCN-LIP-PAC were characterized by conducting the determination of particle size, polydispersity index, zeta potential, and *in vitro* dissolution studies.

#### Particle size and zeta potential analysis

The mean particle size, polydispersion index (PDI), zeta potential of LIP-PAC and BCN-LIP-PAC were measured using dynamic light

scattering with a SZ-100Z (Horiba Scientific, Japan) at  $25\text{ }^\circ\text{C}$ . To prevent multiple scattering phenomena caused by interparticle interactions, the sample dispersion was diluted with ultrapure water for 20 times prior to measurements [21]. At least three times, each sample was measured.

#### Morphological analysis

Transmission electron microscopy JEM-2001 (JEOL, Japan) was used to examine the shape and surface morphology of LIP-PAC and BCN-LIP-PAC (0.1 and 0.3% BCN). In summary, ultrapure water was utilized to dilute the sample dispersion, resulting in a very dilute suspension for TEM imaging [21]. Carefully dropping 8  $\mu\text{l}$  of the sample suspension onto a clean copper grid was done after diluting and air-drying it for 2 min at room temperature after removing excess solution with a filter paper. A 2% aqueous phosphotungstic acid solution (pH = 6.0) was used to carry out negative contrast staining and then air-dried for 2 min at room temperature after removing excess solution with a filter paper. At room temperature, the copper grids were dried before being imaged by TEM.

#### Determination of encapsulation efficiency

Dialysis bags were used to determine the encapsulation efficiency (EE) of LIP-PAC and BCN-LIP-PAC indirectly [21]. To ensure the membrane was completely wet before dialysis, the dialysis membranes were stored overnight in the dissolution medium. The unencapsulated PAC was extracted from the samples by filling them (5 ml) into a dialysis bag (MWCO: 12 000-14 000) and dialysis against 250 ml of deionized water at room temperature for 24 h. The dialysate was analyzed with a UV-Vis spectrophotometer (UV-Vis 2450, Shimadzu, Japan) at 227 nm, which is the absorption maximum for PAC to determine the absorbance of PAC in it. A standard curve between 3 and 10  $\mu\text{g/ml}$  was used to determine the PAC concentration ( $\mu\text{g/ml}$ ) in the dialysate, which corresponded to the regression equation  $y = 0.065664x - 0.000031$  (where  $y$  is the absorbance of the PAC solution and  $x$  is the concentration of the PAC;  $R^2 = 0.9993$ ). The EE was calculated according to Equation 1.

$$EE (\%) = \frac{(Q_t - Q_d)}{Q_t} \times 100\% \dots \dots (1)$$

where EE is the encapsulation efficiency,  $Q_t$  is the theoretical amount of added PAC and  $Q_d$  is the amount of the dialyzed PAC. At least three times, each experiment was repeated.

#### Stability studies in simulated gastrointestinal fluids

The physical-chemical stability of LIP-PAC and BCN-LIP-PAC was investigated in two simulated gastrointestinal fluids: a simulated gastric fluid (SGF, pH 1.2) and a simulated intestinal fluid (SIF, pH 6.8). In SGF and SIF, respectively, 1 ml of the formulations was added to 9 ml of simulated gastrointestinal fluids, and the mixture was subsequently incubated for 2 and 6 h [27, 28]. Particle size, zeta potential, and encapsulation efficiency were assessed as stated for each formulation at either the start or end time.

#### *In vitro* dissolution studies

Membrane dialysis at  $37\text{ }^\circ\text{C}$  was used to evaluate the *in vitro* release of PAC from PAC solution, LIP-PAC, and BCN-LIP-PAC. To ensure proper wetting of the membrane during dialysis, the dialysis membranes (MWCO: 12 000-14 000) were kept overnight in the dissolution medium. Simulated gastrointestinal fluid (SGF, SIF) was used for the *in vitro* release studies for 24 h [21, 27, 28, 36]. To produce the SGF, 2.0 g of NaCl, 7.0 ml of HCl 36-38% and 3.2 g of pepsin were mixed in 1 l of water and the pH was adjusted to 1.2 with 1.0 M HCl. SIF preparation involved adding 6.8 g of  $\text{KH}_2\text{PO}_4$ , 10 g of pancreatin, and 5.0 g of bile salts to 1 l of water and then adjusting the pH to 6.8 with 1.0 mg NaOH. The dissolution test apparatus fixed with eight rotating paddles (Agilent 708-DS Dissolution Apparatus, Malaysia) was utilized to test dissolution. In short, 2 ml of each sample mixed with 2 ml of each aqueous receptor medium were placed in the dialysis bag, which was hermetically sealed and dropped into 200 ml of the aqueous receptor medium and kept at  $37 \pm 0.1\text{ }^\circ\text{C}$  under a stirring rate of 100 rpm. The fresh solution was replaced with 10 ml aliquots of the solution at known time intervals (0, 1, 2, 4, 6, 8, 10, 12, and 24 h) to maintain the total

volume of 200 ml. The withdrawn solution was applied to determine the PAC of the release medium using a UV-Vis spectrophotometer (UV-Vis 2450, Shimadzu, Japan) at a wavelength of 227 nm. The dialysate's PAC concentration ( $\mu\text{g/ml}$ ) was ascertained in the manner mentioned. Equation 2 illustrates how the cumulative release ratio (CR) of PAC from the samples was determined [21, 22, 36].

$$\text{CR (\%)} = \frac{C_1 \times V_1 + \sum_{i=1}^{n-1} C_i \times V_2}{m} \times 100\% \dots\dots (2)$$

Where  $n$  is the number of samples removed from the release medium,  $V_2 = 10$  ml,  $C_i$  is the concentration of PAC in the buffer solutions at time,  $V_1$  is the volume of buffer solution at different pH values (200 ml), and  $m$  is the initial total amount of PAC in the samples.

### Kinetics and mechanism of drug release

Several kinetic models were applied to the analysis of *in vitro* drug release data in order to determine the drug release process. DDSolver, an Excel add-in extension, was used to determine the values of various kinetic models [38]. By fitting release data to various release kinetic models, including zero order, first order, Higuchi, Hixson-Crowell, and Korsmeyer-Peppas equations, the mechanism of PAC release from LIP-PAC or BCN-LIP-PAC was determined. To determine which model best fit the data on release kinetics, such as the correlation coefficient ( $R^2$ ) and release exponent ( $n$ ), calculations were made [4, 21, 27, 28].

### Data analysis and statistics

The mean $\pm$ SD (standard deviation) of all the outcomes from the aforementioned experiments is displayed in the fig. and tables. Using DDSolver, an add-in extension for Microsoft Excel [38], and Analysis ToolPak in Microsoft Excel 2016, the one-way ANOVA test was used to assess the differences between the groups. If there are statistically significant differences, the  $p$ -value is less than 0.05. At least three replications of each experiment were conducted.

**Table 1: Characteristics of nanoliposomes containing paclitaxel (LIP-PAC) and 0.033 % or 0.1 % or 0.3 % bacterial cellulose nanofibers-coated nanoliposomes containing paclitaxel (BCN-LIP-PAC) (All values are expressed as mean $\pm$ SD,  $n = 3$ )**

Formulations	Diameter (nm)	PDI	Zeta potential (mV)	EE (%)
LIP-PAC	112 $\pm$ 4.2	0.21 $\pm$ 0.02	59.5 $\pm$ 3.2	80.6 $\pm$ 2.3
BCN-LIP-PAC (0.033 % BCN)	1280 $\pm$ 169.1	0.73 $\pm$ 0.20	15.7 $\pm$ 3.1	81.9 $\pm$ 1.4
BCN-LIP-PAC (0.1 % BCN)	154 $\pm$ 6.4	0.23 $\pm$ 0.01	37.0 $\pm$ 2.6	84.6 $\pm$ 1.7
BCN-LIP-PAC (0.3 % BCN)	215 $\pm$ 11.8	0.58 $\pm$ 0.06	23.7 $\pm$ 4.5	85.4 $\pm$ 2.1

### Encapsulation efficiency

Table 1 illustrates the effect of coating of bacterial cellulose nanofibers on the PAC encapsulation efficiency of the prepared LIP. The encapsulation efficiency of PAC was 80.6, 81.9, 84.6 and 85.4 % in LIP-PAC, BCN-LIP-PAC (0.033 % BCN), BCN-LIP-PAC (0.1 % BCN) and BCN-LIP-PAC (0.3 % BCN), respectively.

### Morphological observation

The morphology of LIP-PAC and BCN-LIP-PAC (0.1 % or 0.3 % BCN) was confirmed by TEM, as shown in fig. 1. LIP-PAC and BCN-LIP-PAC (0.1 % or 0.3 % BCN) had a nearly spherical morphology and well-dispersed. Coating of bacterial cellulose nanofibers on the LIP-PAC

## RESULTS AND DISCUSSION

### Preparation, optimization and characterization of LIP-PAC and BCN-LIP-PAC

First, nanoliposomes containing paclitaxel (LIP-PAC) were prepared by thin film hydration followed by extrusion method. Subsequently, bacterial cellulose nanofibers-coated nanoliposomes containing paclitaxel (BCN-LIP-PAC) were formed by coating bacterial cellulose nanofibers (BCN) on the surface of LIP-PAC via electrostatic interaction between the positively charged LIP [27, 28] and negatively charged BCN [34], respectively.

The average particle size, polydispersity index (PDI) and zeta potential of LIP-PAC and BCN-LIP-PAC (0.033 % or 0.1 % or 0.3 % BCN) are listed in table 1. LIP-PAC had average particle size and zeta potential of 112 nm and 59.5 mV, respectively. The average sizes and zeta potentials of nanoliposomes formulation coated with different amounts of BCN are also shown in table 1. The particle sizes of BCN-LIP-PAC were found to increase gradually as the amount of BCN increased. In addition, the zeta potential of LIP-PAC was decreased from 59.5 mV to 15.7 mV after BCN coating, which demonstrated that BCN was successfully coated on the surface of nanoliposomes. The increase in particle size and the decrease in zeta potential of BCN-LIP-PAC reflected changes in the nanoliposomes surface properties due to BCN-LIP-PAC interactions.

The average diameter of LIP-PAC, BCN-LIP-PAC (0.033 % BCN), BCN-LIP-PAC (0.1 % BCN) and BCN-LIP-PAC (0.3 % BCN) was 112, 1280, 154 and 215 nm, respectively. We observed that BCN-LIP-PAC (0.033 % BCN) had the largest diameter. This can be explained by the interaction between LIP-PAC and BCN, which caused a greater bilayer expansion in the nanoliposomes. The PDI of LIP-PAC and BCN-LIP-PAC (0.1 % BCN) was 0.21 and 0.23, respectively. This indicates that particle size was well controlled, with a narrow dispersity, since the PDI value is  $<0.3$ . We found that the PDI of BCN-LIP-PAC is slightly greater than LIP-PAC.

does not alter the spherical shape. According to fig. 1, the average size of LIP-PAC, BCN-LIP-PAC (0.1%), and BCN-LIP-PAC (0.3%) is estimated to be roughly 110, 150, and 210 nm, respectively. This value is in good agreement with the results of dynamic light scattering analysis found in table 1.

According to earlier research, liver parenchymal cells filter out nanoparticles smaller than 70 nm from the systemic circulation, whereas particles larger than 300 nm build up in the spleen. The optimal size range for achieving the highest blood concentration of liposomes has been found to be between 70 and 200 nm [21, 37]. Based on the previously mentioned outcomes, LIP-PAC and BCN-LIP-PAC (0.1%) were selected as the ideal formulations for additional research.

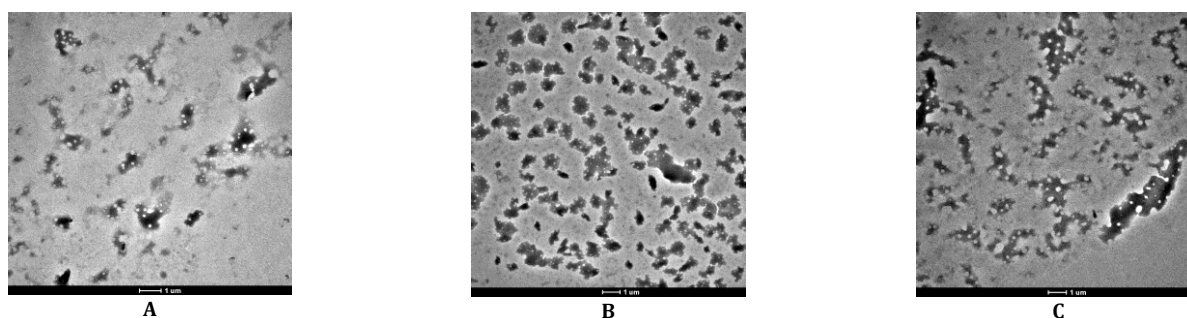


**Fig. 1: TEM of nanoliposomes containing paclitaxel (LIP-PAC) (A); 0.1 % (B), and 0.3 % (C) bacterial cellulose nanofibers-coated nanoliposomes containing paclitaxel (BCN-LIP-PAC); TEM scale bar is 1000 nm**

### Stability studies

LIP instability resulting from aggregation and disintegration in the GI environment is the main constraint for LIP oral administration. Effective oral drug administration thus depends on increasing the stability of drug-loaded LIP in the GI. There have been several attempts to alter LIP using polymers in order to stabilize them and enable their use in oral distribution [21]. The results in table 2 shows the enhanced stability and protective effects of BCN coating on the surface of LIP incubated in SGF and SIF. When incubated in SGF and SIF, the particle size of LIP-PAC increased with time, indicating that it was unstable in the GI environment. This observation may be explained by the possibility that positively charged LIP may adsorb with negatively charged materials in the GI environment, which would cause LIP to become unstable and aggregate. Furthermore, bile salts and other surfactants found in the

GI tract have a major impact on the structural stability of LIP. Additionally, pancreatic lipases break down phospholipids, which might lead to the instability of LIP [21, 27, 28]. Therefore, the disruptive effects mentioned above may have combined to cause the shape, size, and drug loss of LIP-PAC in SGF and SIF that are seen in table 2. When incubated in SGF and SIF, BCN-LIP-PAC particle size dropped somewhat with time. This might be because BCN partially shields the LIP surface in the GI environment. Moreover, the results in our study were also shown that in SGF and SIF, BCN-LIP-PAC exhibited comparatively higher stability when compared to LIP-PAC. This result could be explained by the surface BCN coating's combination shielding action, which produced a stable LIP structure. Table 2 illustrates how BCN-LIP-PAC's shielding action prevented drug leakage from the LIP and phospholipid exposure to the hostile GI environment. Additionally, BCN-LIP-PAC showed reduced PAC loss than LIP-PAC incubated in SGF and SIF.

**Table 2: Stability studies of LIP-PAC and BCN-LIP-PAC in simulated gastrointestinal fluids at 37 °C (All values are expressed as mean±SD, n = 3)**

Parameters	Size (nm)		Zeta potential (mV)		Encapsulation efficiency (%)	
	Initial	Final	Initial	Final	Initial	Final
LIP-PAC						
SGF pH 1.2	112±4.2	148±9.5	59.5±3.2	45.6±3.9	80.6±2.3	27.5±3.5
SIF pH 6.8	112±4.2	175±7.8	59.5±3.2	33.3±4.2	80.6±2.3	22.5±4.3
BCN-LIP-PAC						
SGF pH 1.2	154±6.4	151±7.0	37.0±2.6	40.3±3.3	84.6±1.7	77.0±2.9
SIF pH 6.8	154±6.4	148±2.6	37.0±2.6	41.0±4.5	84.6±1.7	76.3±2.3

### Evaluation of *in vitro* drug release

Using a dynamic dialysis method, the release behavior of the PAC solution, LIP-PAC, and BCN-LIP-PAC was examined in the simulated gastrointestinal conditions (SGF, pH 1.2, and SIF, pH 6.8) [4, 21, 27, 28]. The *in vitro* PAC release curves of PAC solution, LIP-PAC, and BCN-LIP-PAC are shown in fig. 2 and fig. 3. As can be observed, PAC solution showed a rapid-release profile, whereas LIP-PAC and BCN-LIP-PAC demonstrated a slow-release performance.

Fig. 2 and fig. 3 show the *in vitro* release profiles of PAC from LIP-PAC and BCN-LIP-PAC in a gastric digestion simulation environment. The outcomes showed that LIP effectively shielded the encapsulated PAC from pepsin action. In LIP-PAC or BCN-LIP-PAC, more than 70% of PAC was held during the four-hour simulated gastric digestion. For

LIP-PAC or BCN-LIP-PAC, the percentage of drug release in the simulated gastric fluid (SGF) decreased, which is a desired property to shield the bioactive molecule from the harsh gastric environment [21]. Particularly for BCN-LIP-PAC, which had a maximum PAC release of 23.54% in the simulated gastric environment after four hours of incubation, the release profiles of PAC during gastric incubation showed a slight decrease (as shown in fig. 2). The PAC release rate from LIP-PAC is shown in fig. 3, where it was observed to be higher in simulated intestinal fluid (SIF), a combination of bile salts and pancreatin, than in SGF, as reported in other studies [21, 27, 28]. The liposomal surface can be altered to increase their stability within the body [15, 20-29]. A potential alteration is chitosan coating, which can enhance LIP stability in SGF and SIF as well as their mucoadhesive and encapsulated drug solubility [20-26].

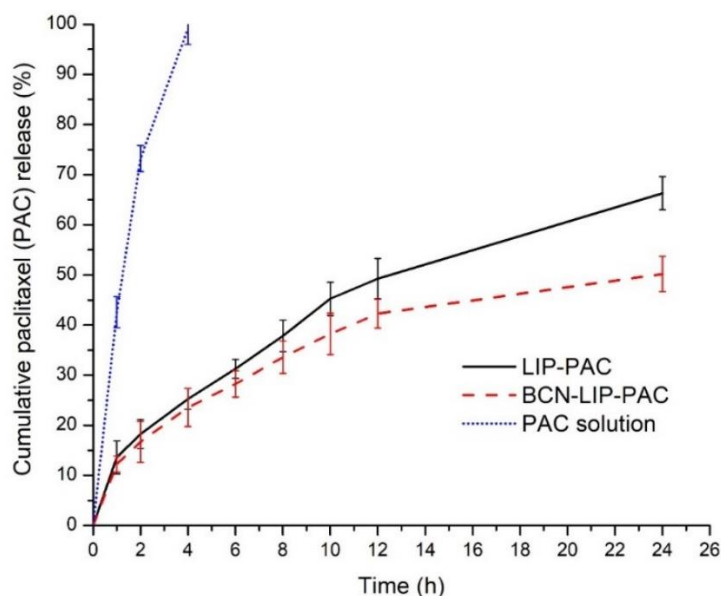


**Fig. 2: *In vitro* PAC release profiles for LIP-PAC, BCN-LIP-PAC and PAC solution in SGF at 37 °C (Results are expressed as mean±SD, n=3)**

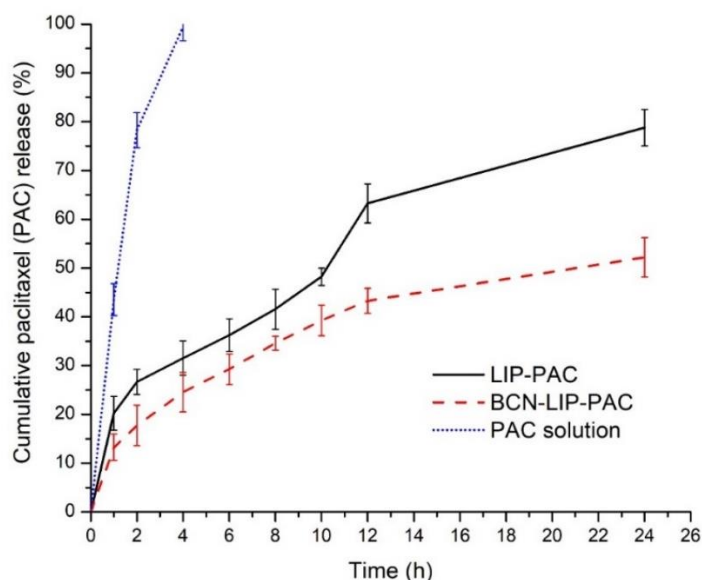


Fig. 3: *In vitro* PAC release profiles for LIP-PAC, BCN-LIP-PAC and PAC solution in SIF at 37 °C (Results are expressed as mean±SD, n=3)

The results presented in fig. 2 and fig. 3 also indicate that PAC solution released over 70 % of PAC at the first 2 h in both SGF and SIF, whereas LIP-PAC and BCN-LIP-PAC released over 18 % and 16 % of PAC, respectively. In addition, the PAC solution released PAC completely in both SGF and SIF in less than 6 h. But, the accumulative PAC releases from LIP-PAC and BCN-LIP-PAC in SGF at 6 h were approximately 31 % and 28 %, respectively; the accumulative PAC releases from LIP-PAC and BCN-LIP-PAC in SIF at 6 h were approximately 36 % and 29 %, respectively. The faster PAC release profile of LIP-PAC might be contributed to the instability behavior in GI conditions. The PAC release profile of LIP-PAC was faster BCN-LIP-PAC in both SGF and SIF. The results indicated that LIP-PAC might be contributed to the instability behavior in GI conditions.

According to the results above, the PAC release profile in the GI tract

was markedly slowed down by the BCN coating on the surface of the nanoliposomes. Additional evidence was presented to support the idea that BCN coating offered a practical means of enhancing nanoliposome stability in the GI.

#### Kinetics and mechanism of drug release

To characterize the kinetic behavior of the drug release mechanism from the formulations, the PAC release profiles of the LIP-PAC and BCN-LIP-PAC were fitted into zero order, first order, Higuchi, Hixson-Crowell, and Korsmeyer-Peppas models; the most appropriate model is the one that best fits the experimental data. Table 3 and table 4 provide an overview of the correlation coefficient values that were determined using drug release kinetics based on different LIP-PAC and BCN-LIP-PAC dissolution models.

Table 3: Values of correlation coefficient ( $R^2$ ) and release exponent ( $n$ ) from LIP-PAC and BCN-LIP-PAC in SGF at 37 °C

Formulations	Correlation of coefficient ( $R^2$ )					(n)	Release mechanism
	Zero-order	First order	Higuchi	Hixson-crowell	Korsmeyer-peppas		
LIP-PAC	0.6867	0.9324	0.9942	0.8859	0.9949	0.519	Non-Fickian diffusion
BCN-LIP-PAC	0.4573	0.7701	0.9899	0.6896	0.9870	0.431	Fickian diffusion

The BCN-LIP-PAC followed Higuchi kinetics, while the LIP-PAC followed Korsmeyer-Peppas kinetics with high linearity in both SGF and SIF medium. Diffusion and erosion are the mechanisms of drug release from LIP-PAC, as evidenced by the observation that the drug release kinetics of LIP-PAC agrees well with the Korsmeyer-Peppas model ( $n > 0.45$ , suggesting Non-Fickian diffusion as a mechanism of

drug release) [4, 21]. The drug release profiles of BCN-LIP-PAC, on the other hand, show that diffusion from matrix systems may be the mechanism of drug release, as they agree well with Higuchi-type drug release kinetics [21]. Previous literature has reported comparable outcomes using particulate nanocarriers based on polymeric aniline (PAC) [27, 28].

Table 4: Values of correlation coefficient ( $R^2$ ) and release exponent ( $n$ ) from LIP-PAC and BCN-LIP-PAC in SIF at 37 °C

Formulations	Correlation of coefficient ( $R^2$ )					(n)	Release mechanism
	Zero-order	First order	Higuchi	Hixson-crowell	Korsmeyer-peppas		
LIP-PAC	0.6142	0.9007	0.9721	0.8635	0.9725	0.486	Non-Fickian diffusion
BCN-LIP-PAC	0.4469	0.7731	0.9914	0.6908	0.9907	0.426	Fickian diffusion

#### CONCLUSION

In this study, bacterial cellulose nanofibers-coated nanoliposomes containing paclitaxel (BCN-LIP-PAC) was successfully prepared, characterized, and evaluated for use in oral drug delivery. The results demonstrated that bacterial cellulose nanofibers was

attached to the surface of nanoliposomes via electrostatic attraction. LIP-PAC and BCN-LIP-PAC (0.1 % BCN) were formed with vesicle sizes in the nano-range,  $112 \pm 4.2$  nm and  $154 \pm 6.4$  nm, and EE % of  $80.6 \pm 2.3$  % and  $84.6 \pm 1.7$  %, respectively. BCN-LIP-PAC was found to be stable in simulated gastrointestinal fluids. According to the analysis of the PAC release profiles of BCN-LIP-PAC in SGF and SIF,

BCN-LIP-PAC showed the sustained PAC release in both SGF and SIF. PAC release from BCN-LIP-PAC was found to follow Higuchi model and Fickian diffusion sustained drug release mechanism. Moreover, the PAC release rate from all LIP-PAC and BCN-LIP-PAC was higher in SIF than in SGF. In conclusion, this kind of BCN-LIP-PAC could be regarded as promising carriers for oral delivery for anticancer compound, PAC.

#### ACKNOWLEDGMENT

The Vietnamese Ministry of Education and Training provided financial support for this study (grant number B.2022-SP2-06), for which the authors are grateful.

#### FUNDING

Nil

#### AUTHORS CONTRIBUTIONS

All the authors contributed equally.

#### CONFLICT OF INTERESTS

There are no conflicts of interest, according to the authors.

#### REFERENCES

1. Thanki K, Gangwal RP, Sangamwar AT, Jain S. Oral delivery of anticancer drugs: challenges and opportunities. *J Control Release*. 2013;170(1):15-40. doi: 10.1016/j.jconrel.2013.04.020, PMID 23648832.
2. Mei L, Zhang Z, Zhao L, Huang L, Yang XL, Tang J. Pharmaceutical nanotechnology for oral delivery of anticancer drugs. *Adv Drug Deliv Rev*. 2013;65(6):880-90. doi: 10.1016/j.addr.2012.11.005, PMID 23220325.
3. Bhosale RR, Janugade BU, Chavan DD, Thorat VM. Current perspectives on applications of nanoparticles for cancer management. *Int J Pharm Pharm Sci*. 2023;15(11):1-10. doi: 10.22159/ijpps.2023v15i11.49319.
4. Huang L, Chen X, Nguyen TX, Tang H, Zhang L, Yang G. Nanocellulose 3D-networks as controlled-release drug carriers. *J Mater Chem B*. 2013;1(23):2976-84. doi: 10.1039/c3tb20149j, PMID 32260865.
5. Tatode AA, Patil AT, Umekar MJ, Telange DR. Investigation of effect of phospholipids on physical and functional characterization of paclitaxel liposomes. *Int J Pharm Pharm Sci*. 2017;9(12):141-6. doi: 10.22159/ijpps.2017v9i12.20749.
6. Lee E, Lee J, Lee IH, Yu M, Kim H, Chae SY. Conjugated chitosan as a novel platform for oral delivery of paclitaxel. *J Med Chem*. 2008;51(20):6442-9. doi: 10.1021/jm800767c, PMID 18826299.
7. Pandita D, Ahuja A, Lather V, Benjamin B, Dutta T, Velpandian T. Development of lipid-based nanoparticles for enhancing the oral bioavailability of paclitaxel. *AAPS PharmSciTech*. 2011;12(2):712-22. doi: 10.1208/s12249-011-9636-8, PMID 21637945.
8. Zhao L, Feng SS. Enhanced oral bioavailability of paclitaxel formulated in vitamin E-TPGS emulsified nanoparticles of biodegradable polymers: *in vitro* and *in vivo* studies. *J Pharm Sci*. 2010;99(8):3552-60. doi: 10.1002/jps.22113, PMID 20564384.
9. Sharma S, Verma A, Pandey G, Mittapelly N, Mishra PR. Investigating the role of pluronic-g-cationic polyelectrolyte as functional stabilizer for nanocrystals: impact on paclitaxel oral bioavailability and tumor growth. *Acta Biomater*. 2015;26:169-83. doi: 10.1016/j.actbio.2015.08.005, PMID 26265061.
10. Li Y, Chen Z, Cui Y, Zhai G, Li L. The construction and characterization of hybrid paclitaxel-in-micelle-in-liposome systems for enhanced oral drug delivery. *Colloids Surf B Biointerfaces*. 2017;160:572-80. doi: 10.1016/j.colsurfb.2017.10.016, PMID 29028605.
11. Tatode AA, Patil AT, Umekar MJ. Application of response surface methodology in optimization of paclitaxel liposomes prepared by thin film hydration technique. *Int J App Pharm*. 2018;10(2):62-9. doi: 10.22159/ijap.2018v10i2.24238, doi: 10.22159/ijap.2018v10i2.24238.
12. Jang Y, Ko MK, Park YE, Hong JW, Lee IH, Chung HJ. Effect of paclitaxel content in the DHP107 oral formulation on oral bioavailability and antitumor activity. *J Drug Deliv Sci Technol*. 2018;48:183-92. doi: 10.1016/j.jddst.2018.09.014.
13. Du X, Khan AR, Fu M, Ji J, Yu A, Zhai G. Current development in the formulations of non-injection administration of paclitaxel. *Int J Pharm*. 2018;542(1-2):242-52. doi: 10.1016/j.ijpharm.2018.03.030, PMID 29555439.
14. Bose P, Kumar De P, Samajdar G, Das D. A strategic process development and *in vitro* cytotoxicity analysis of paclitaxel-loaded liposomes. *Int J App Pharm*. 2023;15:219-27. doi: 10.22159/ijap.2023v15i2.47305, doi: 10.22159/ijap.2023v15i2.47305.
15. Nguyen TX, Huang L, Gauthier M, Yang G, Wang Q. Recent advances in liposome surface modification for oral drug delivery. *Nanomedicine (Lond)*. 2016;11(9):1169-85. doi: 10.2217/nmm.16.9, PMID 27074098.
16. Estanqueiro M, Amaral MH, Conceicao J, Lobo JMS. Evolution of liposomal carriers intended to anticancer drug delivery: an overview. *Int J Curr Pharm Res*. 2015;7(4):26-33.
17. Rodrigues P, Thacker K, Bhupendra GP. Exploring lipid-based drug delivery in cancer therapy via liposomal formulations. *Asian J Pharm Clin Res*. 2022;15(5):15-22. doi: 10.22159/ajpcr.2022.v15i5.43668.
18. Li Z, Zhang M, Liu C, Zhou S, Zhang W, Wang T. Development of liposome containing sodium deoxycholate to enhance oral bioavailability of itraconazole. *Asian J Pharm Sci*. 2017;12(2):157-64. doi: 10.1016/j.ajps.2016.05.006, PMID 32104325.
19. Bohsen MS, Tychsen ST, Kadhim AAH, Grohganz H, Treusch AH, Brandl M. Interaction of liposomes with bile salts investigated by asymmetric flow field-flow fractionation (AF4): a novel approach for stability assessment of oral drug carriers. *Eur J Pharm Sci*. 2023;182:106384. doi: 10.1016/j.ejps.2023.106384, PMID 36642346.
20. Shin GH, Chung SK, Kim JT, Joung HJ, Park HJ. Preparation of chitosan-coated nanoliposomes for improving the mucoadhesive property of curcumin using the ethanol injection method. *J Agric Food Chem*. 2013;61(46):11119-26. doi: 10.1021/jf4035404, PMID 24175657.
21. Nguyen TX, Huang L, Liu L, Elamin Abdalla AM, Gauthier M, Yang G. Chitosan-coated nano-liposomes for the oral delivery of berberine hydrochloride. *J Mater Chem B*. 2014;2(41):7149-59. doi: 10.1039/c4tb00876f, PMID 32261793.
22. Liu Y, Liu D, Zhu L, Gan Q, Le X. Temperature-dependent structure stability and *in vitro* release of chitosan-coated curcumin liposome. *Food Res Int*. 2015;74:97-105. doi: 10.1016/j.foodres.2015.04.024, PMID 28412008.
23. Cuomo F, Cofelice M, Venditti F, Ceglie A, Miguel M, Lindman B. *In vitro* digestion of curcumin loaded chitosan-coated liposomes. *Colloids Surf B Biointerfaces*. 2018;168:29-34. doi: 10.1016/j.colsurfb.2017.11.047, PMID 29183647.
24. Tai K, Rappolt M, Mao L, Gao Y, Li X, Yuan F. The stabilization and release performances of curcumin-loaded liposomes coated by high and low molecular weight chitosan. *Food Hydrocoll*. 2020;99:105355. doi: 10.1016/j.foodhyd.2019.105355.
25. Moslehi M, Mortazavi SAR, Azadi A, Fateh S, Hamidi M, Foroutan SM. Preparation, optimization and characterization of chitosan-coated liposomes for solubility enhancement of furosemide: a model BCS IV drug. *Iran J Pharm Res*. 2020;19(1):366-82. doi: 10.22037/ijpr.2019.111834.13384, PMID 32922494.
26. Zhou W, Cheng C, Ma L, Zou L, Liu W, Li R. The formation of chitosan-coated rhamnolipid liposomes containing curcumin: stability and *in vitro* digestion. *Molecules*. 2021;26(3):560. doi: 10.3390/molecules26030560, PMID 33494543.
27. Jain S, Kumar D, Swarnakar NK, Thanki K. Polyelectrolyte stabilized multilayered liposomes for oral delivery of paclitaxel. *Biomaterials*. 2012;33(28):6758-68. doi: 10.1016/j.biomaterials.2012.05.026, PMID 22748771.
28. Chen MX, Li BK, Yin DK, Liang J, Li SS, Peng DY. Layer-by-layer assembly of chitosan stabilized multilayered liposomes for paclitaxel delivery. *Carbohydr Polym*. 2014;111:298-304. doi: 10.1016/j.carbpol.2014.04.038, PMID 25037355.
29. Yazdi JR, Tafaghodi M, Sadri K, Mashreghi M, Nikpoor AR, Nikoofal Sahlabadi S. Folate targeted pegylated liposomes for the oral delivery of insulin: *in vitro* and *in vivo* studies. *Colloids Surf B Biointerfaces*. 2020;194:111203. doi: 10.1016/j.colsurfb.2020.111203, PMID 32585538.

30. Yamazoe E, Fang JY, Tahara K. Oral mucus-penetrating pegylated liposomes to improve drug absorption: differences in the interaction mechanisms of a mucoadhesive liposome. *Int J Pharm.* 2021;593:120148. doi: 10.1016/j.ijpharm.2020.120148, PMID 33290871.
31. Wu H, Nan J, Yang L, Park HJ, Li J. Insulin-loaded liposomes packaged in alginate hydrogels promote the oral bioavailability of insulin. *J Control Release.* 2023;353:51-62. doi: 10.1016/j.jconrel.2022.11.032, PMID 36410613.
32. He Y, Huang Y, Xu H, Yang X, Liu N, Xu Y. Aptamer-modified M cell targeting liposomes for oral delivery of macromolecules. *Colloids Surf B Biointerfaces.* 2023;222:113109. doi: 10.1016/j.colsurfb.2022.113109, PMID 36599185.
33. Islam MU, Ullah MW, Khan S, Shah N, Park JK. Strategies for cost-effective and enhanced production of bacterial cellulose. *Int J Biol Macromol.* 2017;102:1166-73. doi: 10.1016/j.ijbiomac.2017.04.110, PMID 28487196.
34. Singhsa P, Narain R, Manuspiya H. Bacterial cellulose nanocrystals (BCNC) preparation and characterization from three bacterial cellulose sources and development of functionalized BCNCs as nucleic acid delivery systems. *ACS Appl Nano Mater.* 2018;1(1):209-21. doi: 10.1021/acsanm.7b00105.
35. Badshah M, Ullah H, Khan SA, Park JK, Khan T. Preparation, characterization and in-vitro evaluation of bacterial cellulose matrices for oral drug delivery. *Cellulose.* 2017;24(11):5041-52. doi: 10.1007/s10570-017-1474-8.
36. Nguyen TX, Pham MV, Cao CB. Development and evaluation of oral sustained-release ranitidine delivery system based on bacterial nanocellulose material produced by *Komagataeibacter xylinus*. *Int J App Pharm.* 2020;12(3):48-55. doi: 10.22159/ijap.2020v12i3.37218.
37. Litzinger DC, Buiting AM, van Rooijen N, Huang L. Effect of liposome size on the circulation time and intraorgan distribution of amphipathic poly(ethylene glycol)-containing liposomes. *Biochim Biophys Acta.* 1994;1190(1):99-107. doi: 10.1016/0005-2736(94)90038-8, PMID 8110825.
38. Zhang Y, Huo M, Zhou J, Zou A, Li W, Yao C. DDSolver: an add-in program for modeling and comparison of drug dissolution profiles. *AAPS J.* 2010;12(3):263-71. doi: 10.1208/s12248-010-9185-1, PMID 20373062.